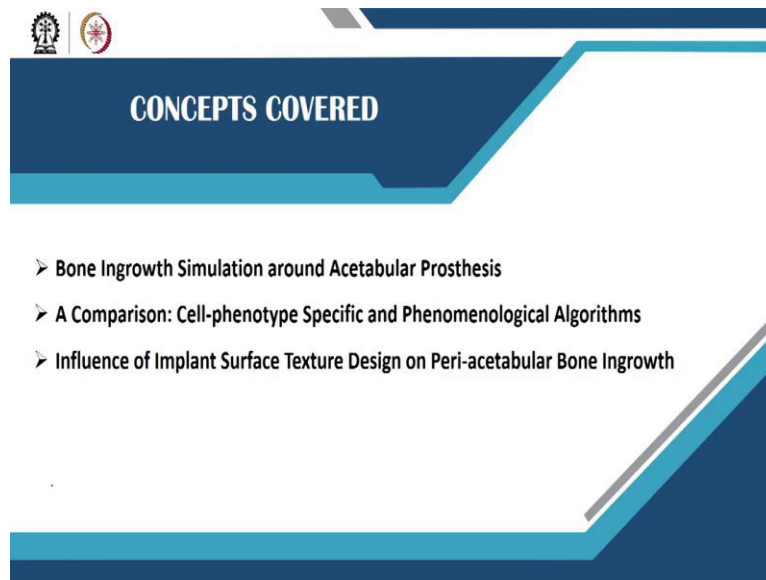


Biomechanics of Joints and Orthopaedic Implants
Professor Sanjay Gupta
Department of Mechanical Engineering
Indian Institute of Technology, Kharagpur
Lecture 43

Tissue Differentiation around Porous Coated Acetabular Implant

Good afternoon everybody. Welcome to the fifth lecture of Module 8 Tissue Differentiation around Porous Coated Acetabular Implant.

(Refer Slide Time: 00:40)



Now in this lecture, we will be discussing three topics. The first topic is bone ingrowth simulation around the acetabular prostheses. After that we will compare the predictions of cell-phenotype specific and phenomenological algorithms, mechanoregulatory algorithms. And finally, we will discuss the influence of implant surface texture design on the peri-acetabular bone ingrowth.

(Refer Slide Time: 01:20)

Peri-Prosthetic Bone Ingrowth

- Cementless implants rely on biological fixation with bone.
- Bone ingrowth is known to follow the principle of fracture healing.
- Over the last two decades, mechanoregulatory algorithms have been developed to quantitatively assess the tissue differentiation.

Motivation

It is necessary to gain an insight into the predictions of peri-prosthetic bone ingrowth by two commonly used mechanoregulatory tissue differentiation algorithms:

- Phenomenological
- Cell-phenotype specific

Figure adapted from www.eorthopod.com

NPTEL Online Certification Courses
IIT Kharagpur

The success of long-term fixation of an uncemented acetabular component depends on the biological fixation with the host bone, which relies on sufficient bone ingrowth around the prosthesis. So cementless implants rely on the biological fixation with bone, and bone ingrowth is known to follow the principle of fracture healing. So during the last two decades, mechanoregulatory algorithms have been developed to quantitatively assess tissue differentiation.

Now bone grows into the porous coating and create a mechanical interlock, eventually helping a secure, eventually helping to secure fixation of the implant with the host bone as shown in the figure presented in the slide.

Now in our laboratory, we set out to investigate peri-acetabular tissue differentiation on an implanted pelvic bone. So before I go into the details, let me state the motivation of the study undertaken in our laboratory. It is necessary to gain an insight into the predictions of peri-prosthetic bone ingrowth by two commonly used mechanoregulatory tissue differentiation algorithms.

The first one is the phenomenological algorithm and the second one is the cell-phenotype specific algorithm. We are interested in the quantitative assessment of peri-acetabular bone ingrowth in the form of spatial distribution of the new tissue layer formed around the implant.

(Refer Slide Time: 03:49)

Bone Ingrowth Simulation around Acetabular Prosthesis

Using a three-dimensional (3D) microscale FE model representing an implant-bone interface, the objective of the study is to quantitatively compare tissue differentiation predictions of the phenomenological and the cell-phenotype specific algorithms, around a porous coated acetabular component.

Source: <https://www.tcd.ie/mecheng/research/>

Cast-in spherical beaded acetabular component

The study is focused on:

- Acetabular component
- Variation in regional bone material properties across the acetabulum
- Variation in implant-bone relative displacement across the acetabulum

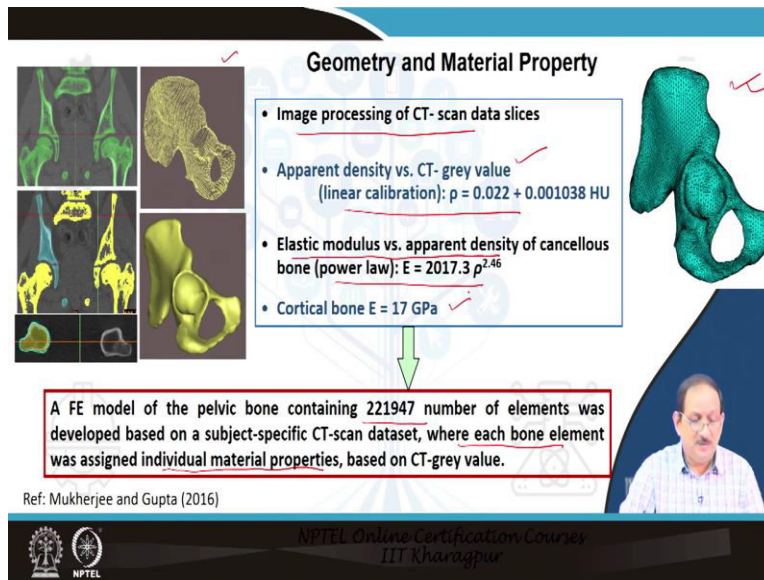
NPTEL Online Certification Courses
IIT Kharagpur

Therefore we set out to investigate bone ingrowth around acetabular components or prosthesis using a three-dimensional microscale FE model representing an implant-bone interface. So the objective was to quantitatively compare tissue differentiation predictions of the two mechanoregulatory algorithms around a porous-coated acetabular component. So as you can see in the slide, we have presented a cast-in spherical beaded acetabular component based on which we have developed the model.

So this is a Birmingham hip resurfacing component, and you can see that the porous coating is in the form of a beaded, spherical beaded structure. The study focuses on the acetabular component and takes into account variation in regional bone material properties across the acetabulum. So this is an essential aspect of the study. It considers the regional variation of bone material properties across the acetabulum and the variation of implant-bone relative displacement across the acetabulum.

So both these two, the bone material property and the implant-bone relative displacement, are expected to vary across the acetabulum. Therefore, it is important to gain an insight into the effect on these two important factors on the effect of these two important factors peri-acetabular tissue differentiation.

(Refer Slide Time: 06:16)



Geometry and Material Property

- Image processing of CT- scan data slices
- Apparent density vs. CT- grey value (linear calibration): $\rho = 0.022 + 0.001038 \text{ HU}$
- Elastic modulus vs. apparent density of cancellous bone (power law): $E = 2017.3 \rho^{2.46}$
- Cortical bone $E = 17 \text{ GPa}$

A FE model of the pelvic bone containing 221947 number of elements was developed based on a subject-specific CT-scan dataset, where each bone element was assigned individual material properties, based on CT-grey value.

Ref: Mukherjee and Gupta (2016)

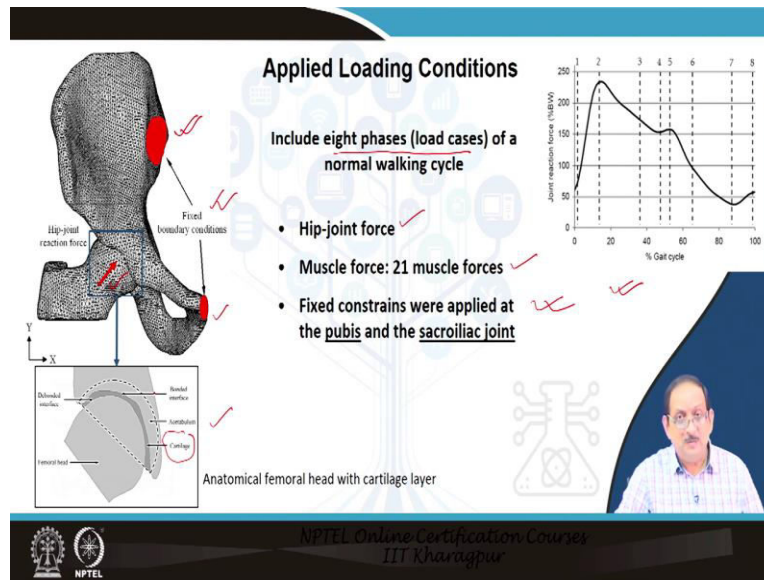
NPTEL Online Certification Courses
IIT Kharagpur

Now let us consider first the development of the Finite Element model. So we developed the Finite Element model based on a CT-scan dataset. So we first undertook the image processing of the CT-scan data slices using the segmentation, thresholding, contour detection, all the steps that are required to generator solid model, from there a Finite Element model as indicated here.

So a Finite Element Model of the pelvic bone containing about 221 thousand elements was developed based on a subject-specific CT-scan dataset, now in which each, now in the FE model, each bone element was assigned individual material properties based on the CT-grey value. We have discussed the procedure in detail earlier. We are just summarizing the salient features of the development of the FE model of the pelvic bone.

So we first relate CT-grey value with apparent density using the linear calibration as indicated here, and then we can relate the elastic modulus with the apparent density of the cancellous bone using the power-law relationship as given here. And then, using these two relationships, each bone element can be assigned individual material properties. So we obtain an FE model of the pelvic bone with heterogeneous bone material properties. However, the cortical bone segmented from the image is assigned to have an E-modulus value or Young's modulus value of 17 Giga Pascal.

(Refer Slide Time: 08:35)

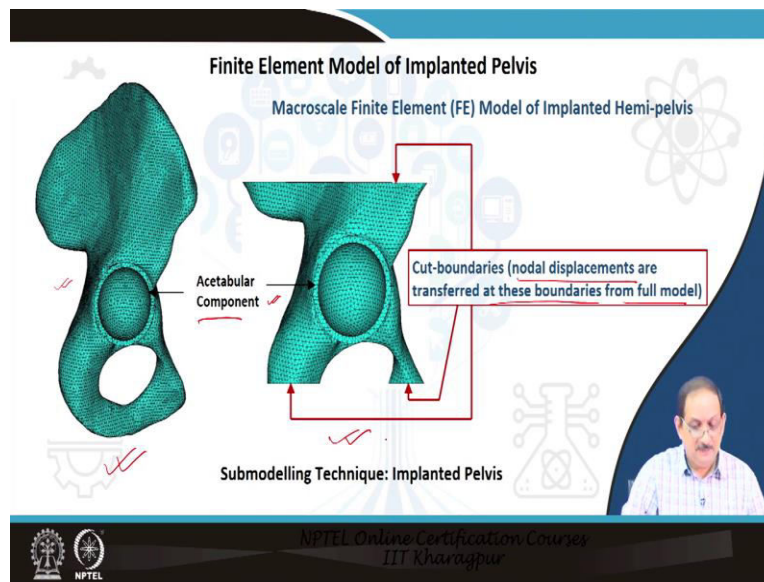


Now let us consider the applied loading conditions used for the simulation. So we are considering 8 phases. So there are 8 load cases, and each load case has a set of musculoskeletal data, consisting of a hip joint force and 21 muscle forces. So each load case has hip joint force data and 21 muscle force data.

So we had divided the Gait cycle into 8 phases as indicated here in the slide, and corresponding to each phase, we have a set of musculoskeletal data of hip joint force and muscle force, 21 muscle force. Then we prescribed the constraints based on the physiological constraints.

So here, you can see that the fixed boundary conditions were prescribed at the pubis and the sacroiliac joint. In this figure, the FE model of the pelvic bone and a part of the femur, proximal femur, as shown in this slide, also contains the hip joint reaction force or hip contact force as given by the red arrow, and we had applied this hip joint reaction force through the femoral head. We considered a cartilage layer as shown here between the acetabulum and the femoral head for the natural pelvic model.

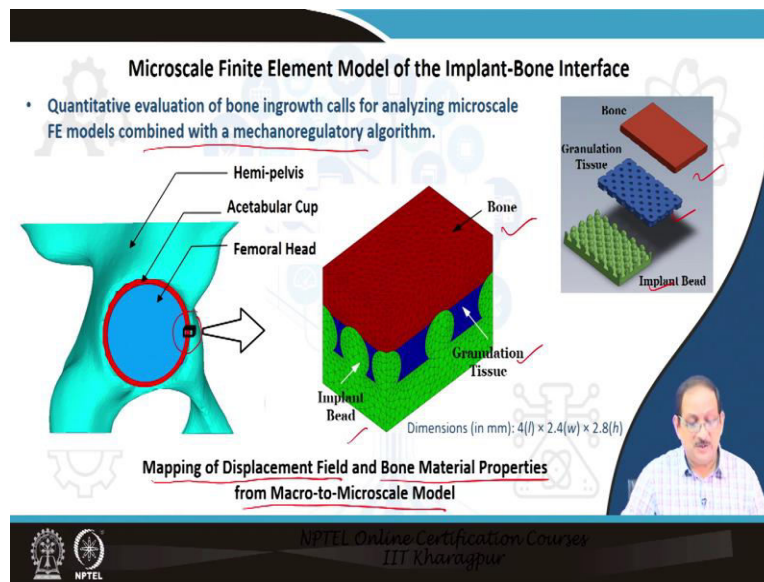
(Refer Slide Time: 10:32)



Now let us move into the macroscale FE model of the implanted hemipelvis. As you can see, on the left, we have a complete model of the pelvic bone with the acetabular component implanted within the FE model. On the right or in the middle of the slide, we have a truncated submodel, which is a fine model compared to the acetabular region of the full-scale model.

Now we are interested in the precise calculation in and around the domain of inclusion of the acetabular prosthesis. So we used a sub modelling technique by which we can transfer the nodal displacements at the cut boundaries from the full-scale model to the submodel. So this ensures that the elastic property of the remaining part of the pelvis is included in the submodel. This sub-modelling technique can include the remaining part of the pelvic bone's elastic behaviour in the implanted pelvis's submodel.

(Refer Slide Time: 12:33)

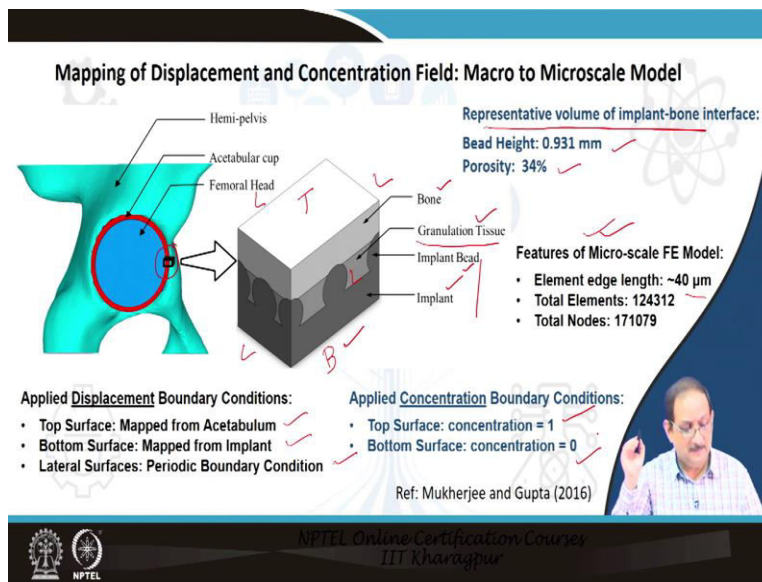


We need a microscale Finite Element model of the implant-bone interface to simulate bone ingrowth in the interfacial area. So a 3D-microscale model has been considered for quantitative evaluation of bone ingrowth combined with mechanoregulatory algorithm.

Now the 3D-microscale model represents only a small portion of the implant-bone interface. It consists of three layers; implant, granulation tissue and bone. Now bone ingrowth around cementless pores coated implants have been simulated employing the mechanoregulatory tissue differentiation algorithms.

In order to simulate the mechanical environment within the microscale model, a mapping framework is developed so that it would link the physiological boundary conditions and the host bone material properties of the macroscale model to the microscale model. So we map the displacement field and the bone material properties from the macro to microscale model. FE simulations can predict spatial distribution of evolutionary tissue differentiation around a prosthesis.

(Refer Slide Time: 14:38)



Let us discuss the mapping of displacements and concentration fields more in detail from the macro to micro-scale model. Now here in this slide, as you can see, we re-introduce the microscale model. So we have the implant and implant bead, granulation tissue and bone. Please note that the granulation tissue is sandwiched between the bone and the implant containing the implant beads. So granulation tissue is located within the inter-bead spacing.

This representative volume of the implant-bone interface in the form of a very small element or a volume has a bead height of 0.31 millimetres and the porosity is 34 percent. The features of the microscale FE model is indicated here, indicating the element edge length of about 40 microns and the total number of nodes and elements.

Now let us move to the boundary conditions. Now in the structural analysis, the displacement boundary conditions can be obtained from the implant-bone relative micromotion of the macroscale model. These implant-bone relative displacements of the macroscale models will be mapped in the microscale model in the following way.

So we have the top surface T, which belongs to the bone. So, on the top surface, the displacements will be mapped from the acetabulum. The bottom surface is the implant. So in the bottom surface, the displacements will be mapped from the implant. On the lateral surface, we prescribe periodic boundary conditions. We prescribe periodic boundary conditions to represent the repetitive nature of the boundary conditions.

The other aspect of boundary conditions is based on the diffusion analysis, which is a separate analysis. So from the diffusion analysis, the top boundary, which belongs to the bone, of the microscale model is considered to have a maximum concentration of 1 since it is the source of mesenchymal stem cells, whereas the bottom surface adjacent to the implant has zero concentration of MSC.

(Refer Slide Time: 18:34)

Tissue Differentiation Predictions: Phenomenological Algorithm

In order to account for the variation in host bone material properties and implant-bone relative displacements, the implanted acetabulum is divided into 13 regions.

Corresponding to each region, a microscale model is developed that includes host bone material properties and local implant-bone relative displacements, using a mapping framework.

Corresponding to each of the 13 macroscale regions of the implanted acetabulum, the average regional elastic modulus is calculated and is assigned to the respective microscale model.

Red: 12-25% BI
Black: 45-55% BI
Purple: 60-70% BI
Blue: 75-90% BI
BI: Bone Ingrowth

NPTEL Online Certification Courses
IIT Kharagpur

Now let us move into the various aspects of this simulation employing a phenomenological algorithm. As you can see in the slide, we have presented here total 13 regions within the acetabulum. Now to account for the variation in host bone material property and implant-bone relative displacements, the implanted acetabulum is divided into 13 regions, as shown in the slide.

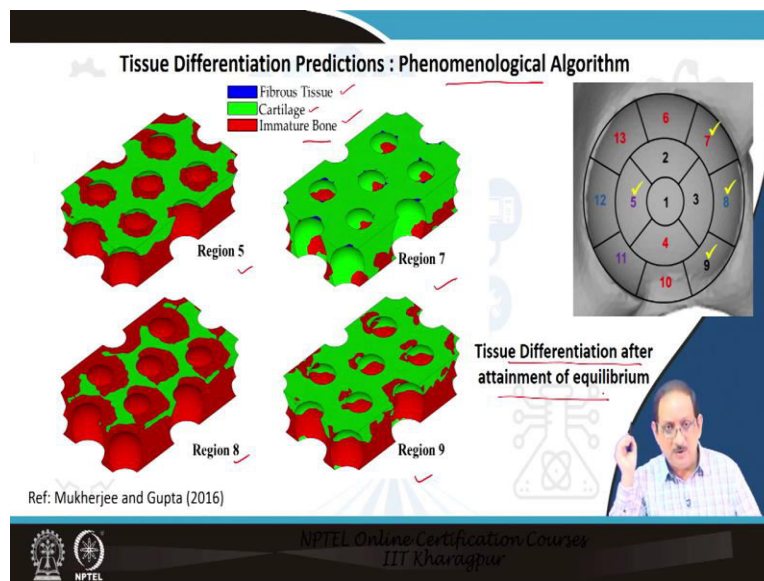
A microscale model is developed considering each region that includes host bone material property and local implant-bone relative displacement using a mapping framework as discussed earlier. Corresponding to each of the 13 macroscale regions of the implanted acetabulum, we have 13 regions of the implanted acetabulum in the microscale model. The average regional elastic modulus is calculated and assigned to the respective microscale model.

Now we present here, based on the results, we have identified a few regions marked in red, black, purple and blue. These colour-coded regions represent a range of bone ingrowth. Say, the regions marked in red, the bone ingrowth varies between 12 to 25 percent. The bone ingrowth ranges

from 45 to 55 percent in the black region, in the purple 60 to 70 percent, and in the blue region 75, the highest 75 to 90 percent.

We have picked up one region from each of these colour-coded regions, and we will present results for each of these selected regions. So we select 5, 7, 8 and 9, which is representative of the entire acetabular region.

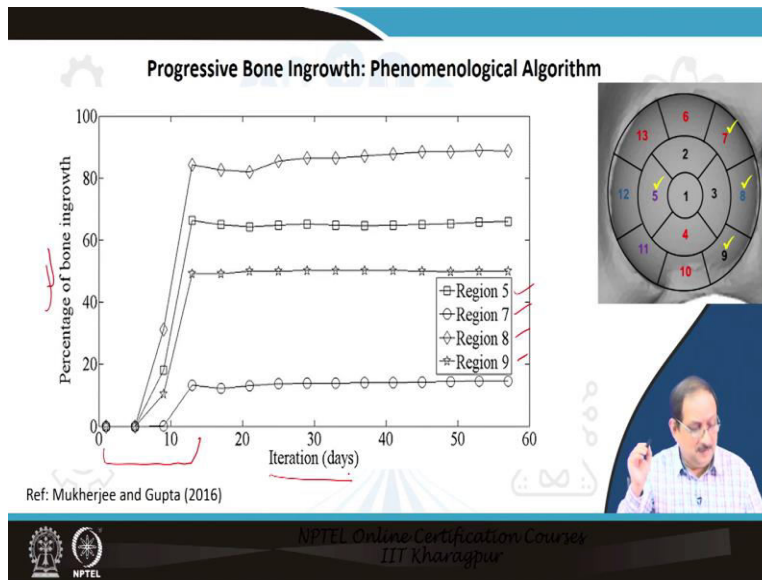
(Refer Slide Time: 21:56)



Now I present to you the results of the spatial distribution of tissue differentiation based on the phenomenological algorithm, and the results are presented for these selected four regions; regions 5, 7, 8 and 9. So here, you can see that the bone ingrowth is maximum in region 8 followed by region 9 and 5, but less in region 7. So from the contour plot the blue region is the fibrous tissue. The cartilage is marked in green colour, and bone, immature bone is red colour.

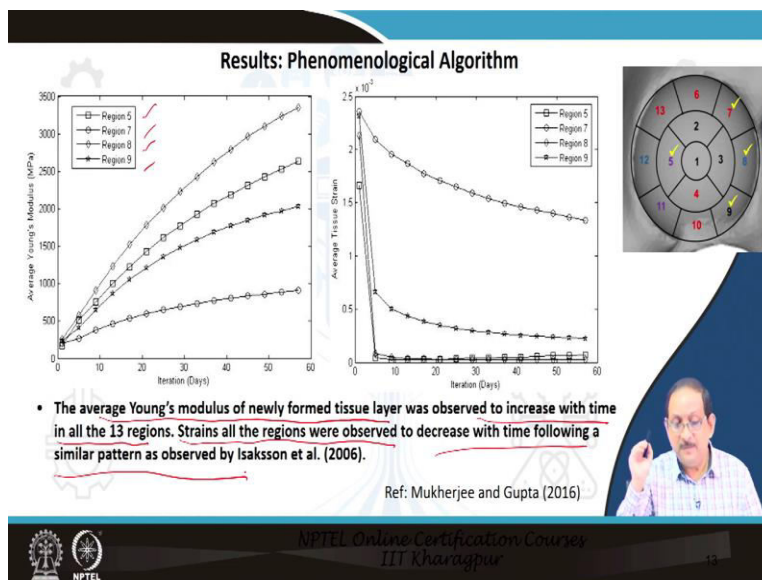
So in region 7 we can see fibrous tissue and cartilage formed mainly in the inter-bead spacing of region 7. So this is the configuration of the tissue differentiation after attainment of equilibrium.

(Refer Slide Time: 23:28)



Now let us present to you the percentage of bone ingrowth in these four regions; regions 5, 7, 8 and 9. As you can observe, in the initial about two weeks, there is a rapid increase in the percentage of bone ingrowth which stabilizes, after that with time as expressed or as indicated here in the figure.

(Refer Slide Time: 24:21)



The time dependent increase of average Young's modulus of the newly formed tissue layer was observed to increase with time in all the 13 regions. Here we have presented only the four regions; 5, 7, 8 and 9. So the average Young's modulus in the newly formed tissue layer is

increasing. At the same time the strains in all the regions were observed to decrease with time following a similar pattern as observed by Isaksson who published the data in 2006.

(Refer Slide Time: 25:19)

Clinical Relevance and Qualitative Validation

Overall FE Predicted Bone Ingrowth : $45.6\% \pm 24.6$ (13-88)
(averaged over 13 regions, single acetabular component)

- Clinical (histological and radiographic) Studies:
 - Hanzlik and Day (2013):
Titanium Acetabular Shell: $46 \pm 20\%$ (20-83)
76 different acetabular components
 - Engh et al. (1993):
Porous Coated Acetabular Implant: 33% (3-84)
9 different acetabular components

Source: Hanzlik and Day (2013), J Arthrop, 28: 922-927

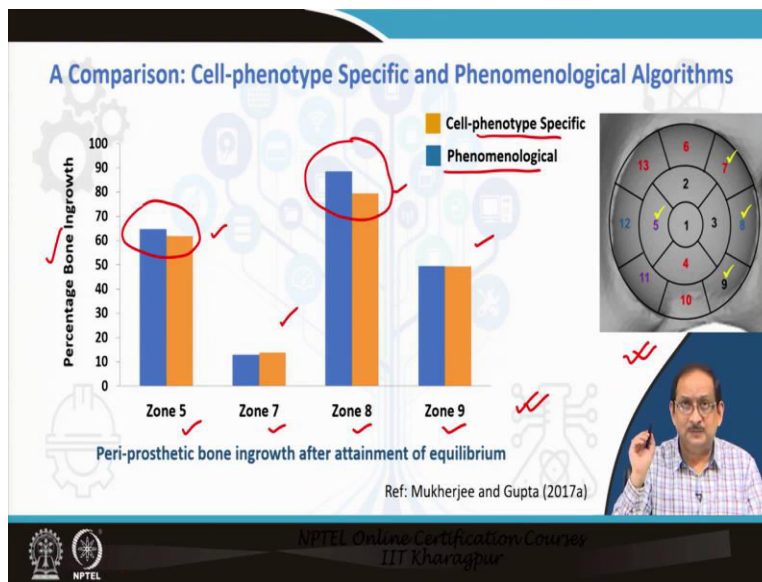
The slide features a histological image on the left showing bone ingrowth into a porous structure, with red lines and numbers 1 through 7 indicating different regions. A small inset photo of a man is visible in the bottom right corner of the slide.

The results need to have some clinical relevance which serves as a qualitative validation as well. The validation is necessary to trust the simulation and give predicted numerical results. Our study predicted an overall bone ingrowth of about 45.6 percent, of course with some variations because we are averaging over 13 regions and corresponding to a single acetabular component. There may be various types of acetabular component design. So we are only presenting the results corresponding to a single subject and a single acetabular component.

But let's look into the clinical studies, in particular the histological and radiographic studies. We see that Titanium acetabular components, in the case of Titanium acetabular components, 76 different acetabular components, the bone ingrowth observed in the histological studies as marked here in the figure by Hanzlik and Day in 2013.

They found 46 percent bone ingrowth in 76 different acetabular components. Of course, there is a variation. The variation is from 20 percent to 83 percent as compared to our variation of 13 percent to 88 percent. The other study predicted about 33, actually observed about 33 percent bone ingrowth varying between 3 to 84 percent for nine different acetabular components.

(Refer Slide Time: 27:55)

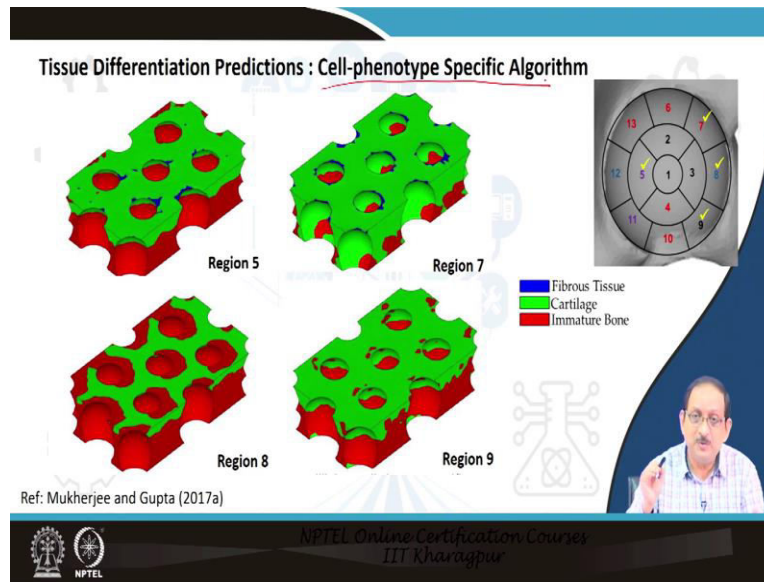


Let us discuss the second topic of this lecture on comparing results predicted by this cell-phenotype-specific and phenomenological algorithms. Now, as you can see in the slide that a bar diagram has been presented. So in this bar diagram, a comparison of the percentage of bone ingrowth around the acetabular component has been presented for four representative regions 5, 7, 8 and 9. And these results correspond to the situation after attainment of equilibrium in the bone tissue ingrowth simulation.

So the blue color corresponds to the results of the phenomenological model, and the orange color corresponds to the results of the cell-phenotype specific model. Now, what do we observe from this figure? In this figure, we plotted a bar diagram of periprosthetic bone ingrowth after attaining equilibrium in the representative four zones.

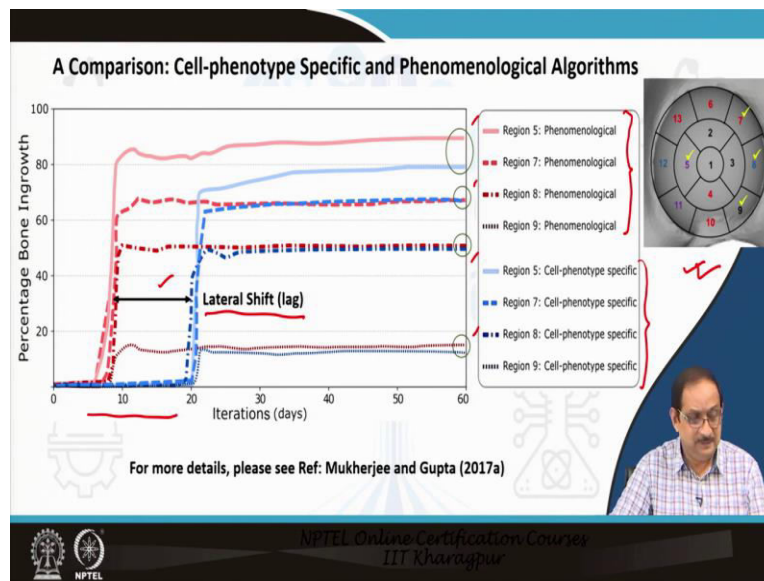
So what do we observe from this figure? The predicted percentages of bone ingrowth after equilibrium that is the end configuration of the simulations in all the four zones are almost similar for both the algorithms. However, in the majority of the 13 peri-acetabular regions, the bone ingrowth predictions were marginally less. Here we are presenting only four zones, but if we consider all the 13 zones, in the majority of the 13 peri-acetabular regions, the bone ingrowth predictions were marginally less for the cell-phenotype specific compared to the phenomenological algorithm.

(Refer Slide Time: 30:43)



Now, if we plot the tissue differentiation, spatial distribution of tissue differentiation corresponding to the cell-phenotype specific algorithm, we see almost a similar distribution compared to the phenomenological algorithm presented earlier.

(Refer Slide Time: 31:07)



Let us now present the progression of bone ingrowth in four representative regions as predicted by the two mechanoregulatory algorithms. Now the pink reddish colour curves correspond to the phenomenological algorithms. So the results are corresponding to the phenomenological

algorithms in regions 5, 7, 8 and 9, whereas the bluish-coloured curves correspond to the results predicted by the cell-phenotype specific algorithms.

Now in most of the 13 peri-acetabular regions, as indicated in the figure on the right, the bone ingrowth predictions were marginally less for the cell-phenotype specific algorithm than the phenomenological algorithm. This is clearly visible in the slide and marked by circles.

Most importantly, however, we observed a lateral shift or lag in the bone ingrowth predictions of the cell-phenotype specific algorithms. The bone ingrowth predictions of cell-phenotype-specific algorithms lag behind those predicted by the phenomenological algorithms, as shown in the figure. This might be due to the values of individual coefficients describing the different cellular activities, which were less than unity. So these different cellular activities in the cell-phenotype specific algorithms were proliferation, differentiation, apoptosis, extracellular matrix formation, and degradation, as discussed earlier in the module.


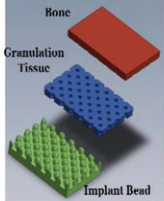
So because of this lag or delay in the process of tissue differentiation, this resulted in a reduced bone ingrowth rate for the cell-phenotype specific algorithm as compared to the phenomenological algorithm. Despite the differences in predicted tissue differentiation patterns during the initial tissue transition period, the overall tissue differentiation patterns after attainment of equilibrium in bone remodelling predicted by these two algorithms were very similar for this study.

(Refer Slide Time: 34:54)

Influence of Implant Surface Texture Design on Peri-acetabular Bone Ingrowth

- Two-level Full Factorial Design of Experiments Method has been implemented.
- Total number of factors: 3
 - Details of design factors:
 - ✓ Bead height: 600 μ m and 900 μ m
 - ✓ Bead diameter: 1000 μ m and 1500 μ m
 - ✓ Inter-bead spacing: 200 μ m and 600 μ m
- Total number of treatment conditions: 8 (= 2³), since two-level full factorial design of experiment has been used.

Ref: Mukherjee and Gupta (2017b)

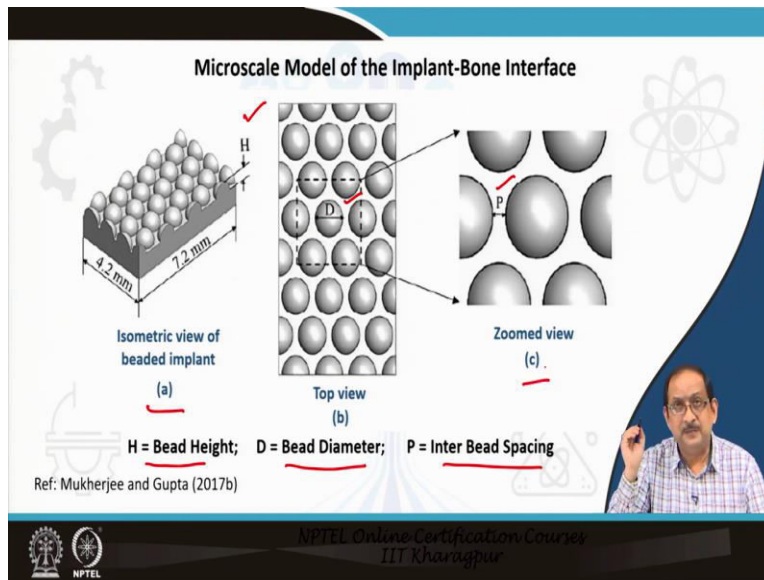


NPTEL Online Certification Courses
IIT Kharagpur

Let us now briefly discuss the third topic, the influence of implant surface texture design on peri-acetabular bone ingrowth. So we are using Two-level Full Factorial Design of experiments method to investigate the influence of surface texture design. There is a total number of three factors. The total number of factors are three, and the detail of the design factors are given here; the bead height, bead diameter and inter bead spacing are the three design factors. And you can see they are varying from 600 micron to 900 micron for the bead height and for the others indicated here in the slide.

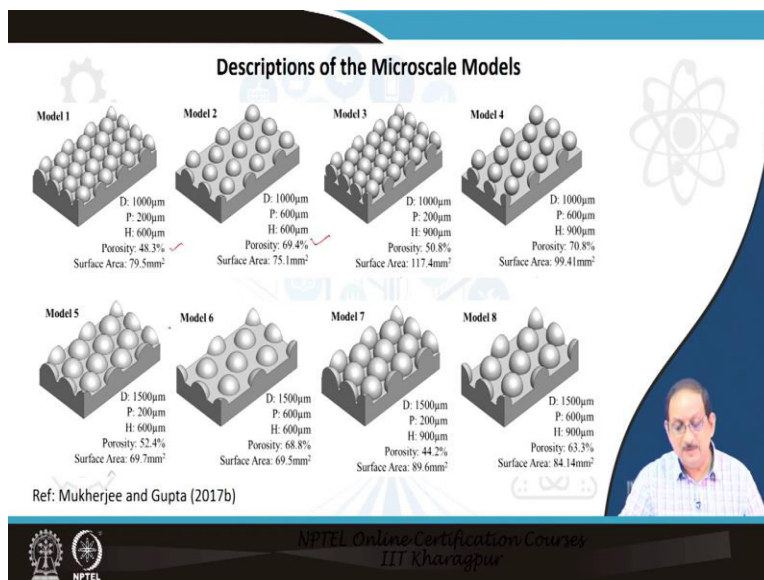
So total number of treatment conditions is 8; since Two-level Full Factorial Design of experiments have been used. So we need 8 models to implement the Two-level Full Factorial Design of experiments method.

(Refer Slide Time: 36:29)



The main design factors the bead height, bead diameter and inter bead spacing as considered in this study, is now presented in this figure. So the bead height is shown in an isometric view of the beaded implant as shown in figure a. The bead diameter is shown in the top view in figure b, and the inter bead spacing P is presented in a closer view or a zoomed view in figure c.

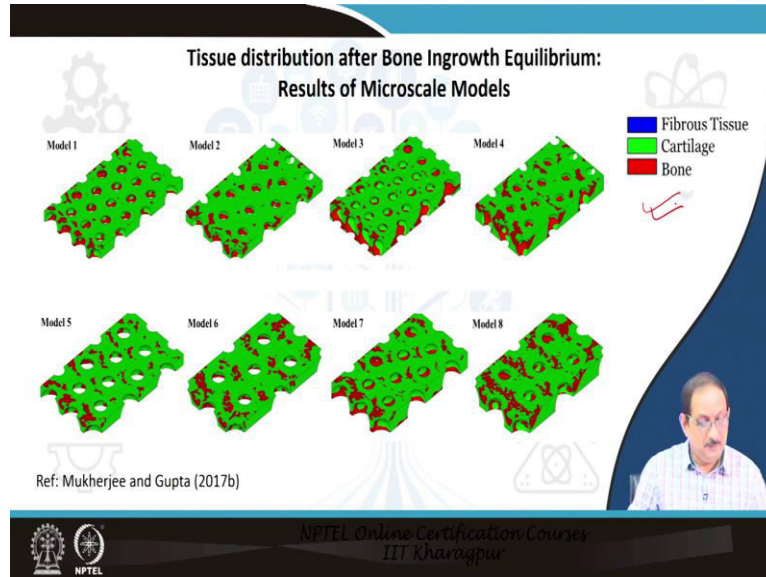
(Refer Slide Time: 37:19)



So now I present to you the 8 models with the descriptions of the individual microscale models, where you can see that the porosity varies because any one of the three factors is varying. It may

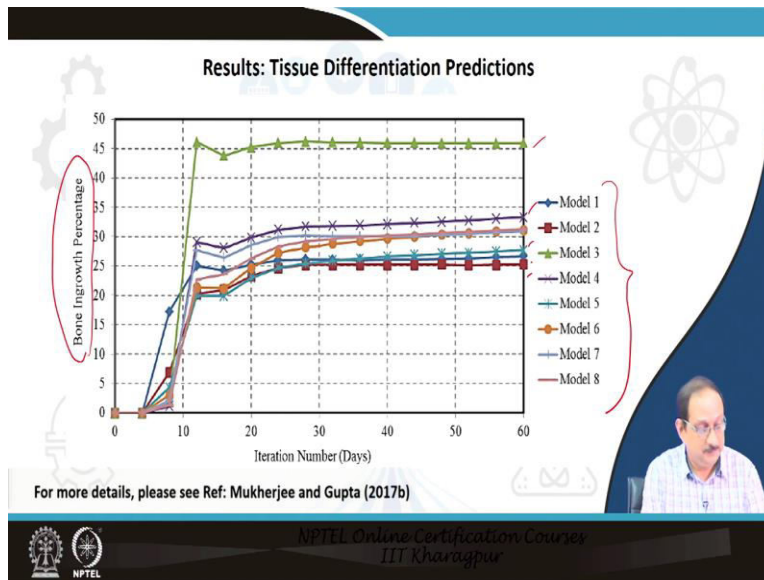
be bead height. It maybe bead diameter. Or it may be inter bead spacing. So a detailed description of the 6 models are presented here in this slide.

(Refer Slide Time: 37:55)



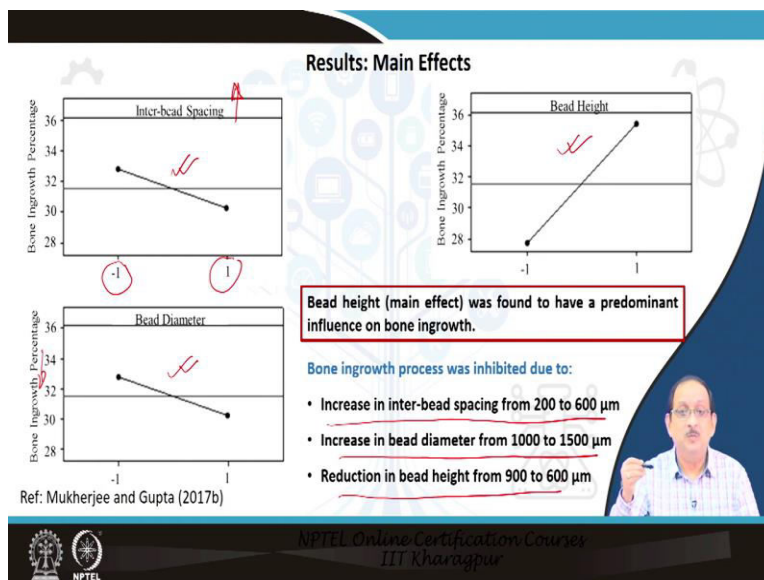
Let us come to the results of the microscale model. After equilibrium of tissue differentiation, the spatial distribution of tissue differentiation is presented here for the 8 models. The tissue differentiation simulation predicts attainment of equilibrium within 2 to 3 postoperative weeks. However, large variations in the quantitative bone ingrowth among these 8 models are noticeable.

(Refer Slide Time: 38:43)



Now, the surface texture design of beaded implants are found to have considerable influence on the peri-implant bone ingrowth. So here in this slide, we have presented the result for all the 8 models. So the bone ingrowth percentage is presented for all the 8 models and you can see that there is variation in the percentage of bone ingrowth corresponding to the 8 models.

(Refer Slide Time: 39:36)



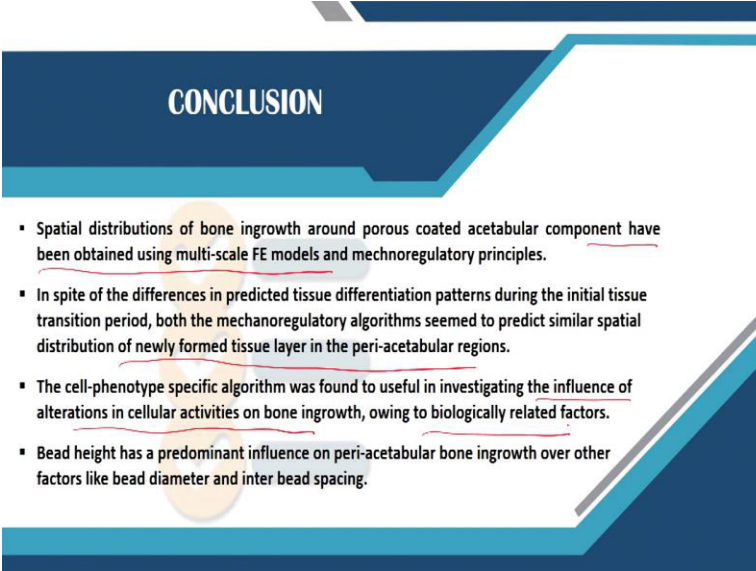
Now which of these three main factors that we have selected is affecting the bone ingrowth and how? Let us look into the Main Effects. Here in this slide, the Main Effects plot of 3 independent factors inter bead spacing, bead height and bead diameter on percentage of bone ingrowth has

been presented. Now, -1 denotes the minimum level, and +1 denotes the maximum level of these factors.

So when inter bead spacing is increasing, the bone ingrowth percentage is decreasing as clearly evident in the first plot. When we are increasing the bead height the bone ingrowth percentage is increasing considerably. Similarly, the bone ingrowth percentage decreases when we increase the bead diameter, as clearly evident in this figure.

So let me summarize that bead height within these three Main Effects was found to have a predominant influence on the bone ingrowth. The bone ingrowth process was inhibited due to an increase in inter bead spacing from 200 to 600 microns, an increase in bead diameter from 1000 to 1500 microns and a reduction in bead height from 900 to 600 microns. So what we understand is that if we increase bead height, it will lead to an increase in bone ingrowth percentage.

(Refer Slide Time: 42:11)



CONCLUSION

- Spatial distributions of bone ingrowth around porous coated acetabular component have been obtained using multi-scale FE models and mechoregulatory principles.
- In spite of the differences in predicted tissue differentiation patterns during the initial tissue transition period, both the mechanoregulatory algorithms seemed to predict similar spatial distribution of newly formed tissue layer in the peri-acetabular regions.
- The cell-phenotype specific algorithm was found to be useful in investigating the influence of alterations in cellular activities on bone ingrowth, owing to biologically related factors.
- Bead height has a predominant influence on peri-acetabular bone ingrowth over other factors like bead diameter and inter bead spacing.

So let me state the conclusions of this lecture. Spatial distributions of bone ingrowth around porous-coated acetabular component have been obtained using multiscale FE models and mechanoregulatory principles or algorithms. Despite the differences in predicted tissue differentiation patterns during the initial tissue transition period, the mechanoregulatory algorithms seem to predict similar spatial distribution of the newly formed tissue layer in the peri-acetabular regions.

The cell-phenotype algorithm or the cell-phenotype specific algorithm was useful in investigating the influence of alterations in cellular activities on bone ingrowth owing to biologically related factors. The bead height predominantly influences peri-acetabular bone ingrowth over other factors like bead diameter and inter bead spacing.

(Refer Slide Time: 43:27)



The list of references are indicated in two slides based on which the lecture has been prepared. Thank you for listening.